

CMS Observation of a narrow resonance at 125 GeV

Joseph Incandela¹

University of California Santa Barbara and CERN

5105 Broida Hall, Santa Barbara, California, USA

Spokesperson, CMS Experiment

E-mail: incandel1@hep.ucsb.edu

The Higgs boson is the quantum of a complex scalar field that is postulated to give mass to W^+ , W^- and Z^0 bosons and to explain the masses of the fundamental quarks and leptons. It has been the target of searches at accelerators around the world for more than a quarter of a century. In the context of a Higgs boson search the Compact Muon Solenoid Collaboration has observed a new particle with a statistical significance of five standard deviations in proton-proton collisions at the Large Hadron Collider at CERN. The evidence is strongest in the diphoton and four-lepton final states, which also have the best mass resolution. The probability for this to be the result of a fluctuation of the background is $\sim 3 \times 10^{-7}$ corresponding to 5σ . The new particle is a boson with spin different from unity and mass $m_x \sim 125$ GeV. Its measured properties are consistent with those expected of the Higgs boson within the uncertainties of the present data. More data are needed to know the precise nature of the new particle.

*36th International Conference on High Energy Physics
July 4-11, 2012
Melbourne, Australia*

¹ *On behalf of the CMS collaboration*

² We do not show particle charges in the remainder of the text.

1. Introduction

The Standard Model (SM) of particle physics [1–3] describes the fundamental fermions and the gauge fields that govern their interactions. Among the gauge bosons that carry the forces in the SM, photons and gluons are massless while the W^\pm and Z^0 have large masses generated by symmetry breaking [4–9] as a result of the introduction of a complex scalar field with a non-zero vacuum expectation value. The model predicts the existence of a new scalar “Higgs” boson. The scalar field also gives mass to the fundamental fermions through a Yukawa interaction [1–3]. In the SM, everything is known about this new boson except its mass, which affects its properties strongly. Theoretical arguments limit m_H to be below ~ 1 TeV [10–13]. Prior searches exclude m_H values below 114.4 GeV [14] and in a narrow region near 160 GeV [15] while the Tevatron reports an excess of events in the range 120–135 GeV [16–18].

The LHC is a circular accelerator, 27 km in circumference and 100 m underground [19]. The LHC has accelerated and collided beams of protons at record energies of $\sqrt{s} = 7$ (8) TeV in 2011 (2012). For the SM Higgs, the production increases with \sqrt{s} and decreases with m_H . The probability of Higgs boson production per proton-proton (pp) collision is $\sim 10^{-10}$. The LHC peak design value at the time of this presentation in July of 2012 is approximately $6.5 \times 10^{33} \text{ cm}^{-2} \text{ s}^{-1}$, achieved with 1368 proton bunches per beam, at 50 ns separation with up to $\sim 1.5 \times 10^{11}$ protons per bunch squeezed to a transverse size of about 20 μm at the interaction point. Each bunch-crossing yields on average 7 (14) pp collisions known as pileup in 2011 (2012) for the data presented here. Pileup is an important challenge for the detectors at the LHC.

In this contribution we report the observation of a new particle whose properties are consistent with those of the SM Higgs boson. We give an overview of the experiment and results that are described in greater detail in Ref. [20]. Five main decay modes are studied involving bosons ($\gamma\gamma$, ZZ , W^+W^-) and the heaviest accessible fermions ($b\bar{b}$, $\tau^+\tau^-$).²

2. Overview of the CMS Detector

The highly modular Compact Muon Solenoid (CMS) detector seen in Figure 1 is used for both proton-proton (pp) and heavy-ion collisions [21]. The detector has a 3.8T superconducting solenoid 13m long, 6m in diameter that houses the silicon pixel and strip tracker, lead tungstate (PbWO_4) scintillating crystal electromagnetic calorimeter (ECAL) and a brass-scintillator hadron calorimeter (HCAL). Muons are identified with gas-ionization detectors in the steel flux-return yoke of the solenoid. Forward calorimeters extend to within 0.8° of the beam axis.

The all-silicon tracker has 66M pixels and 9.3M strips in 13 (11-12) layers in the central (forward) regions for $> 99\%$ tracking efficiency and 1.5-3% p_T resolution at 100 GeV. Decay vertices are reconstructed with high and increasing efficiency and precision as a function of track multiplicity. Electrons and photons produce showers in ECAL’s 75,848 PbWO_4 crystals to yield scintillation light proportional to their energy that’s detected by photo-detectors with a precision of $\sim 1\%$ for the photons and electrons we’ll consider. Similarly, the muon system has transverse momentum (p_T) resolution better than 1% for the muons used in these searches.

² We do not show particle charges in the remainder of the text.

CMS uses a bi-level online trigger system to reduce the event rate from ~ 16 MHz to ~ 500 Hz by selecting events with leptons, photons, jets, high energy (ΣE_T), missing transverse energy (E_T^{miss}) or combinations of these features. Level 1 uses custom electronics to analyze calorimeter and muon information and has an output rate ≤ 95 kHz. The High Level Trigger uses 13,000 processors to study data from all sub-detectors. Billions of events are recorded each year and sent to computing centers around the world for reconstruction and analysis.

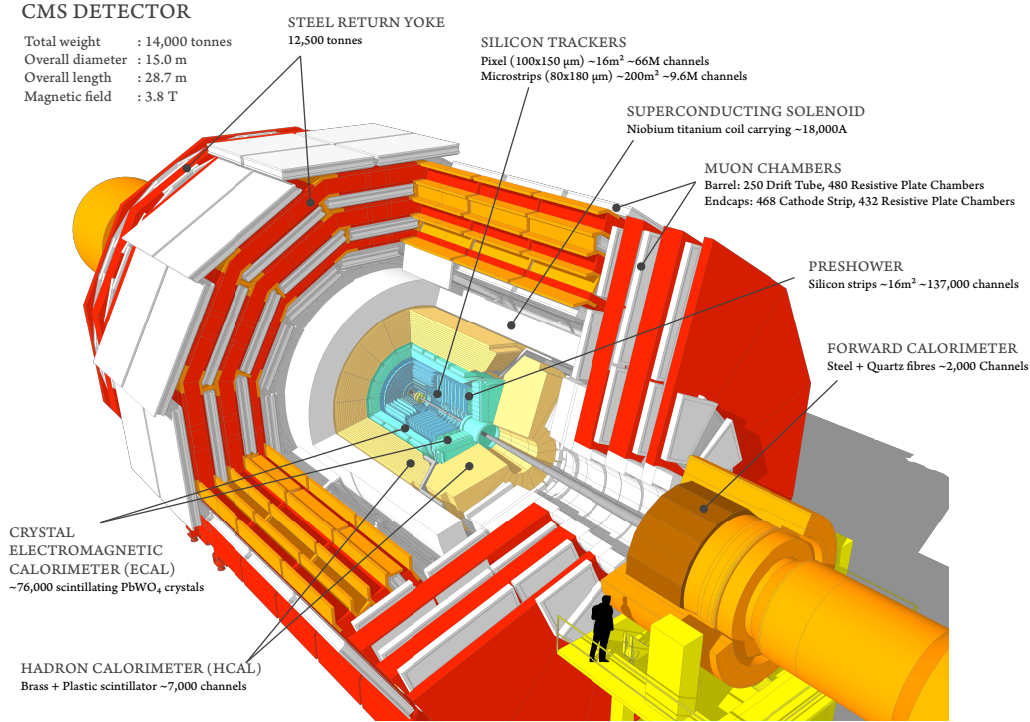


Fig. 1: Schematic view of the CMS Detector showing its main components.

CMS uses a global event description based upon particle flow shown in figure 2 (left). The algorithm uses all CMS detectors to find charged hadrons, muons, electrons, photons and finally neutral hadrons that are used to build more complex objects (e.g. isolated leptons, photons, jets, τ 's, E_T^{miss} ...) with resilience to pileup as seen for low p_T forward electrons in Figure 2 (right).

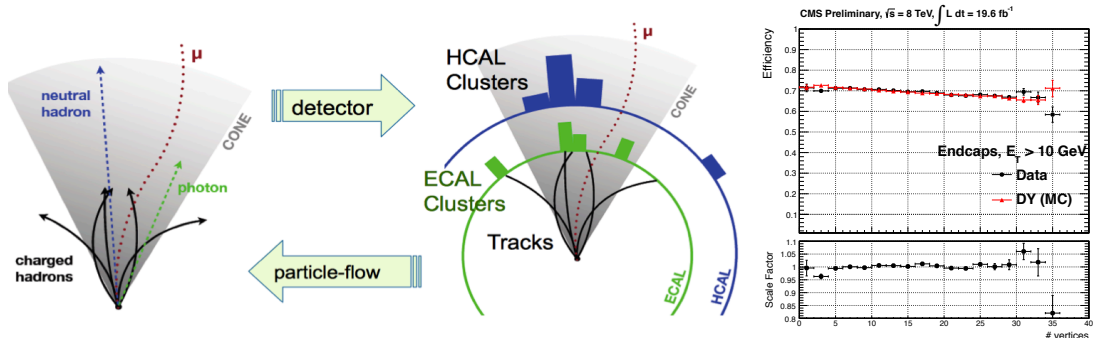


Fig. 2: Left: CMS particle flow. Particles from the pp interaction produce signals in high granularity CMS sub-detectors all of which are used to reconstruct charged hadrons, e, μ , γ , and finally neutral hadrons. Right: Signal efficiency in data (black) versus number of reconstructed pp collisions for forward electrons, $p_T > 10$ GeV, using a particle-flow-based isolation algorithm, compared to Monte Carlo (red).

POS (ICHEP2012)037

3. Searching for the SM Higgs Boson

At the LHC the SM Higgs boson is produced mainly through gluon-gluon fusion followed by vector boson fusion (VBF) and associated production (VH), where $V = W$ or Z . The latter two modes have better signal-to-background (S/B), but have much lower rates [22–26]. VBF events involve high-energy forward jets that can help identify this production mode. SM Higgs bosons are produced at a rate of $\sim 20\text{k}/\text{fb}^{-1}$ for $m_H=125$ GeV. Most however cannot be cleanly identified so we exploit kinematic regions where S/B is large. Large samples of simulated events are used to refine the analysis techniques, estimate backgrounds and predict the expected significance for the observation of new particles [27–30]. Backgrounds are mostly derived from data control samples. In the low mass region the SM Higgs search relies on 5 decay modes: $H \rightarrow \gamma\gamma$, ZZ , WW , $\tau\tau$ and $b\bar{b}$. $H \rightarrow \gamma\gamma$, ZZ , and WW are comparable in sensitivity but the $H \rightarrow \gamma\gamma$ and ZZ channels have excellent mass resolution so that signal would appear as narrow peaks, enabling precise mass determinations. The fermionic decays are very challenging.

In 2011 CMS collected 5.1 fb^{-1} of data at 7 TeV that was used to exclude the mass region between 127 and 600 GeV [31–36]. ATLAS excluded a similar region [37]. Below 127 GeV the data from both experiments showed excesses over background, mainly in the $\gamma\gamma$ channel, near ~ 125 GeV. The excesses were not at all conclusive at $\sim 2\sigma$ once the look-elsewhere effect is taken into account in the 110–145 GeV mass range. The LHC collision energy was raised to 8 TeV in 2012, leading to $\sim 25\%$ increase in SM Higgs boson production in the low mass region. Analysis improvements added 20-30% more sensitivity despite higher pileup. By the summer of 2012, CMS collected 5.3 fb^{-1} data at $\sqrt{s} = 8$ TeV. Given the excesses seen near 125 GeV in 2011 analysis [31–36] and to avoid potential biases, the new data analyses were performed “blind” in the sense that the low mass region was not studied before all analysis criteria were finalized.

3.1 Search for $H \rightarrow \gamma\gamma$

At 125 GeV, the branching ratio $B(H \rightarrow \gamma\gamma)$ is only $\sim 0.3\%$ but $H \rightarrow \gamma\gamma$ is a key mode because the signal appears as a narrow peak above a smooth, steeply falling background in the $\gamma\gamma$ mass distribution. Energy resolution and scale are thus the critical parameters. An *in-situ* ECAL calibration uses $\pi^0, \eta^0 \rightarrow \gamma\gamma$ decays and electrons from W and Z decays. Radiation causes a small, steady loss of transparency in ECAL crystals. This is monitored in real-time by a laser system to obtain corrections enabling a response uniformity of $\pm 0.2\%$ as verified by the E/p ratio for electrons from $W \rightarrow e\nu$ decays. $Z \rightarrow ee$ data are used for the final energy resolutions and scales.

The diphoton mass resolution is not strongly affected by angular resolution of the photon trajectories provided that the interaction point is known to better than ~ 1 cm. This can be a challenge in a high pileup environment, particularly since photons cannot be tracked unless they convert to an e^+e^- pair. To find the correct vertex, a variety of vertex-related information is used such as Σp_T^2 and overall p_T balance of tracks relative to the momentum of the $\gamma\gamma$ system. Information from conversions is also used when it is available. Multivariate analyses [38, 39] based on boosted decision trees (BDT) are used to identify photons and to extract their energies and uncertainties. The full set of selection criteria are provided in ref. [20] for the data

considered here. Events that don't pass VBF selection, as discussed below, are separated into four classes to maximize sensitivity. The classes have successively looser quality criteria as determined by mass resolution, photon kinematics, absence/presence of conversions, isolation etc. Unconverted photons tend to have higher quality and higher S/B for SM Higgs, particularly

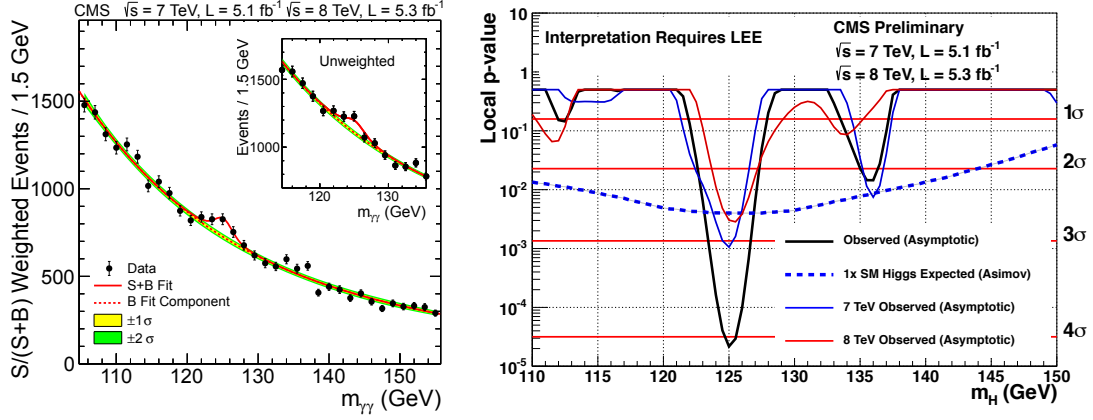


Fig. 3: Left: Combination of $m_{\gamma\gamma}$ event class distributions weighted by $S/(S+B)$ or unweighted (inset). Solid red lines show fits to $S+B$ assuming a 125 GeV SM Higgs. Dashed red lines show background-only with 1 and 2 σ bands in yellow and green, respectively. Right: The observed probability (local p-value) as a function of m_H for the background to fluctuate to the excess observed.

for large $p_T(\gamma\gamma)$. Exclusive VBF classes are defined for events with two relatively high p_T jets with large pseudorapidity separation and large mass. Figure 3 shows the mass spectrum where the event classes are weighted by $S/(S+B)$ and combined or combined without weights (inset). An excess of events is seen at 125 GeV that's consistent with expectations for a SM Higgs. The background mostly involves SM processes producing two real photons. A smaller fraction involves a real photon and a fake photon from a misidentified jet. The background spectrum in each standard class is fit with a 5th order polynomial. A 3rd order polynomial is used for the VBF categories. The magnitude of the excess above the background for all categories combined has a significance of 4.1 σ relative to the background-only hypothesis. Consistent excesses are present in 2011 and 2012 data. A diphoton signal precludes unit spin for the new particle [40, 41].

3.2 Search for $H \rightarrow ZZ^*$

The branching ratio $B(H \rightarrow ZZ^*)$ is $\sim 2.6\%$ for a 125 GeV Higgs where there is at least one off-shell Z . The decays $Z \rightarrow ll$ where $l = e$ or μ have smallest backgrounds, producing $2e2\mu$, $4e$ and 4μ final states. Single and dilepton triggers are used to select events online. Offline selection cuts go down to 5 (7) GeV for μ (e) in $|\eta| < 2.4$ (2.5). The leptons are generally well isolated even in high pileup conditions and can be selected with high efficiency. We require the presence of four isolated leptons that originate from the same interaction vertex.

Selection criteria were honed using a large sample of single- Z events collected in 2011-12. Z boson candidates must decay to same-flavor leptons of opposite charge with mass in the range 40–120 (12–120) GeV for the heavier (lighter) pair. The invariant mass of the ZZ^* system can be determined with good accuracy, allowing the signal to appear as a narrow peak above background. SM background processes include irreducible, non-resonant ZZ^* production which

is estimated via Monte Carlo (MC). Other backgrounds such as individual Z bosons produced in association with heavy-flavor jets and $t\bar{t}$ production are estimated from data.

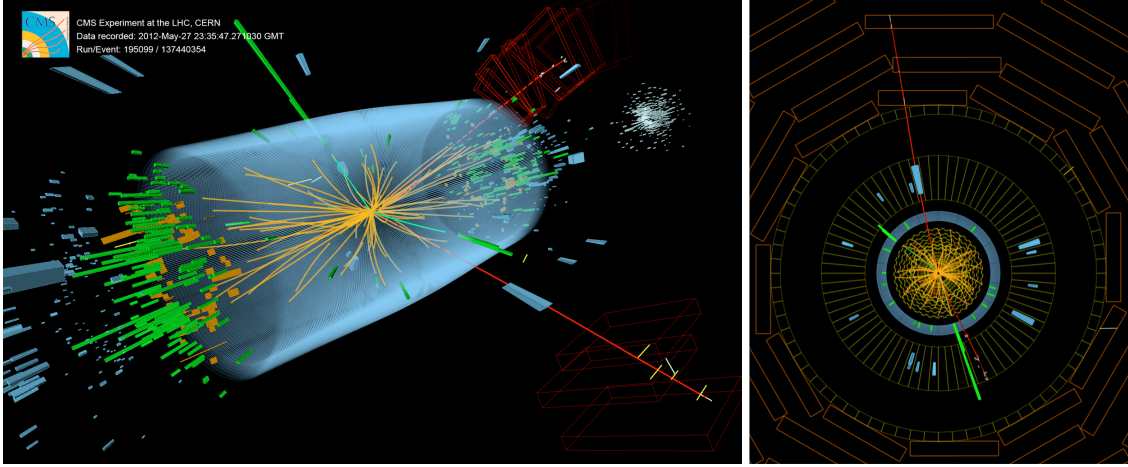


Fig. 4: Three dimensional (left) and transverse (right) views of a candidate $H \rightarrow ZZ$ event recorded at $\sqrt{s} = 8$ TeV with one $Z \rightarrow \mu\mu$ (tracks and towers marked in red) and one $Z \rightarrow ee$ (tracks and towers in green).

Figure 4 shows an event containing two reconstructed Z bosons, with ZZ invariant mass near 125 GeV. The mass spectrum for selected events is shown in Figure 5. A lepton can radiate a photon at an early stage, potentially leading to an underestimate of its energy if this is not taken into account. Photons consistent with final state radiation are thus included in the lepton energy calculation where appropriate. Figure 5 displays a statistically significant peak near 125 GeV. There is also a clear Z peak at 91 GeV from $Z \rightarrow 4l$ where one lepton pair from the conversion of an energetic virtual photon.

Separation of signal from background is improved by exploiting event kinematics, (especially decay angles and invariant masses of the dilepton pairs), in a Matrix Element Likelihood Analysis (MELA) [42]. Events in the peak at 125 GeV are seen in Figure 5 to have a

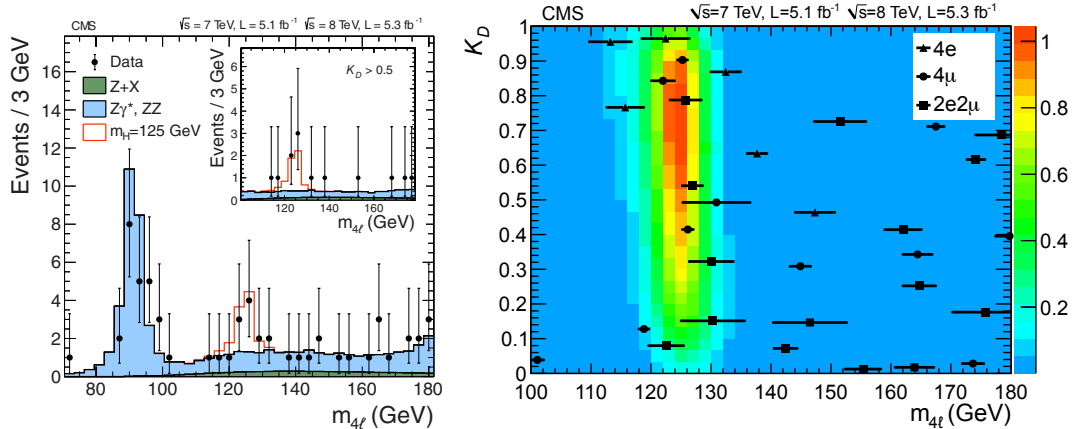


Fig. 5: Left: Invariant mass for $4e$, 4μ and $2e2\mu$ with expectations for background and 125 GeV SM Higgs indicated. The inset shows the m_{4l} distribution after a Matrix Element Likelihood Analysis (MELA), for those events with likelihood discriminator $K_D > 0.5$. Right: Comparison of data to expectation for a 125 GeV Higgs in the 2 dimensional distribution of K_D versus m_{4l} .

higher value of the discriminator K_D as expected for a SM Higgs. The statistical significance of the excess upon taking into account decay-angle characteristics has a maximum of 3.2σ relative to the background-only hypothesis at 125.6 GeV. The SM Higgs expectation is 3.8σ .

3.3 Searches for $H \rightarrow WW, \tau\tau$, and $b\bar{b}$

For $H \rightarrow WW$, the most sensitive final states contain two opposite-sign leptons ($ee, e\mu$ or $\mu\mu$) and significant E_T^{miss} due to the undetected neutrinos. In contrast to the $\gamma\gamma$ and ZZ modes the mass cannot be reconstructed precisely. The signal is therefore expected to appear as an excess over background that extends over a broad mass range. Multivariate analysis techniques are used to optimize the sensitivity to signal. Events are categorized by lepton flavor content and jet multiplicity with different backgrounds and sensitivities. Jet identification and E_T^{miss} require some care in a high pileup environment where energy deposits from multiple pp collisions can become intertwined. Pileup effects are largely neutralized by associating charged particles to their correct interaction vertices and by means of MVA techniques that use jet shape variables to separate real jets from clusters of pileup energy deposits. The final impact of pileup on the correct accounting of events with zero additional jets is negligible, as seen in Figure 6.

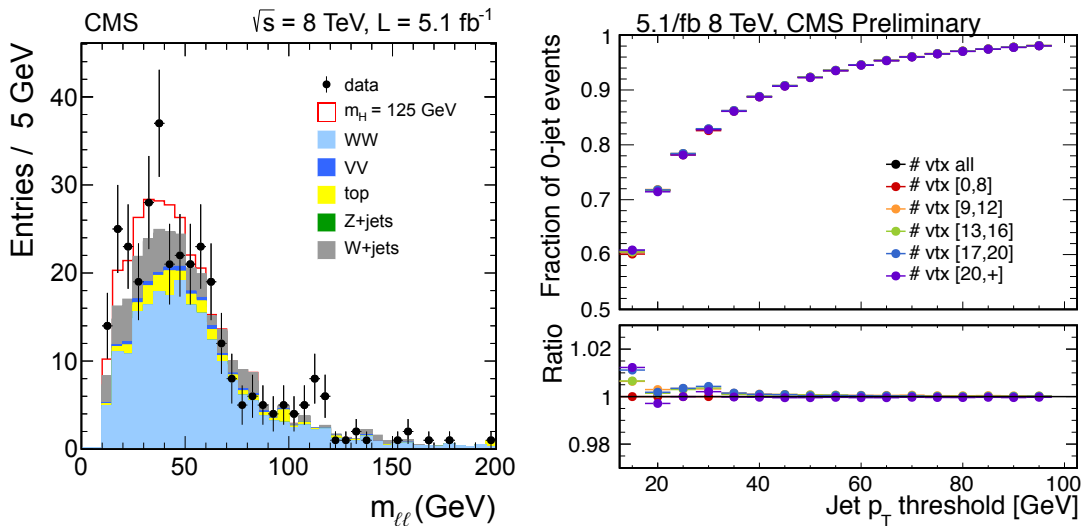


Fig. 6: Left: Invariant mass of lepton pairs for the zero-jet $e\mu$ category in the search for $H \rightarrow WW$ at 8 TeV. The 125 GeV SM Higgs boson signal is shown added to the background. Right: Fraction of events in the 0-jet category as a function of jet p_T for 5 exclusive ranges of the number of reconstructed vertices.

We select events in which the most (2^{nd} most) energetic lepton has $p_T > 20$ (10) GeV and typically $E_T^{\text{miss}} > 20$ GeV. Estimation of SM backgrounds is challenging and generally makes use of data control samples complemented by MC samples to extrapolate into the signal region. Combining all classes from 2011 and 2012 data, we see a broad excess of events at the level of $1.5\text{--}2.0\sigma$ that is consistent with the presence of a new particle at a mass near 125 GeV.

Under the assumption that its coupling is proportional to mass, we search for decays of this new particle to the heaviest accessible fermions – namely pairs of τ leptons and b quarks. The detection of τ leptons is challenging because they have a multitude of decay modes to leptons ($\tau \rightarrow l\nu\bar{\nu}, l = e, \mu$), or to one or three π^\pm , possibly accompanied by π^0 's, and a ν_τ . CMS

reconstructs the leptonic decays and several classes of hadronic decays with good efficiency and low fake rates as verified with $Z \rightarrow \tau\tau$ data [43].

The challenge here is the understanding of the backgrounds. They are mostly extracted using control samples in data. Events are classified by four pairings ($\tau_e\tau_\mu$, $\tau_e\tau_h$, $\tau_\mu\tau_h$, $\tau_\mu\tau_\mu$) of tau decays and by the presence of jets. Again, different classes of events have different backgrounds and signal sensitivities and the presence of neutrinos means that the signal would appear as a broad enhancement over background. No such enhancement was observed in summer 2012.

Finally, CMS conducted a search for SM $H \rightarrow b\bar{b}$. The b quark jets are tagged via displaced vertices. The energy of the original b quark is obtained from the energies of all particles associated with the b jet and has large uncertainty. The $H \rightarrow b\bar{b}$ mass distribution is expected to have a width of ~ 20 GeV for $m_H < 135$ GeV. SM $H \rightarrow b\bar{b}$ has the largest branching fraction of all decays at low mass but the signal for the dominant Higgs production mode is overwhelmed by continuum $b\bar{b}$ background. We therefore search for this signal in the more rare VH production mode with $V = W$ or Z for which events can be easily flagged by the leptonic decays of the W and Z. We also require $p_T^V \geq 50$ GeV. Several mutually exclusive event classes defined by lepton flavor of the associated boson decay and $p_T^{b\bar{b}}$ are used to optimize sensitivity. The result obtained by combining all channels shows a small excess of events above the background-only expectation spanning a large mass range, including the region near 125 GeV. Sensitivity is however inadequate to establish the presence of a signal.

4. Observation of a New Particle

The information for the five search channels is combined in a global fit [44]. Local p-values are evaluated by means of pseudo-experiments made up of simulated data that incorporate all experimental uncertainties and correlations in the different analyses. The results for the individual channels and the combination are shown in Figure 7. The minimum p-value for the combination is at ~ 125 GeV and has a local significance of 5σ , consistent with the expectation of $5.8 \pm 1.0 \sigma$ for SM Higgs. Taking into account look elsewhere effect in the mass range 114–130 GeV yields a global significance of 4.6σ . We have thus observed a new particle!

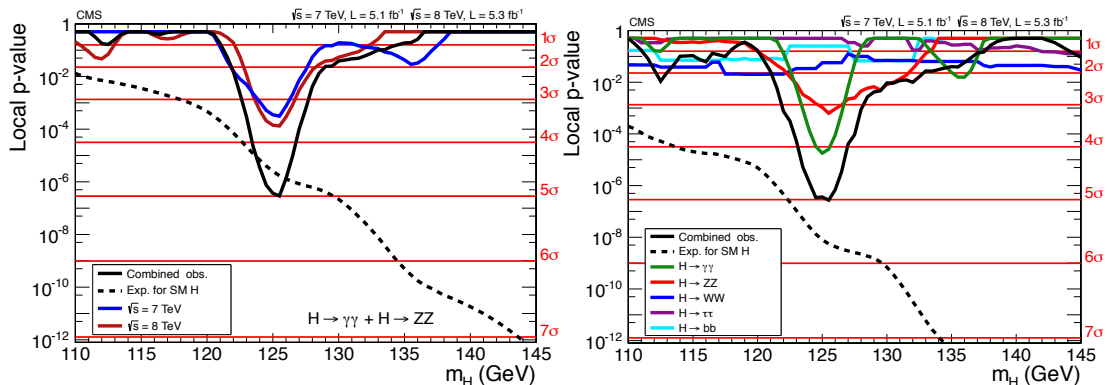


Fig. 7: Left: Local p-values versus m_H for the combination of $H \rightarrow \gamma\gamma$ and $H \rightarrow ZZ^*$ at 7 and 8 TeV separately and combined. Right: Local p-values versus m_H for each of the five search channels individually, and in combination. Dashed lines show the median expectation for the SM Higgs boson.

In addition to establishing the existence of a new particle, we can use our data to extract some of its properties, such as its mass. Moreover, once the mass is known, then all other properties such as the production cross-sections for the various production modes and the branching fractions to various final states are known for the SM Higgs. We can thus probe our data for consistency with the SM Higgs hypothesis. This is done using the measured production rates as determined for each decay mode individually and for the overall combination, each normalized to the corresponding expectation for a SM Higgs boson. The resulting signal strengths indicate that the $\gamma\gamma$ channel is highest at 1.6 ± 0.4 , whereas the value for the ZZ channel is $0.7^{+0.4}_{-0.3}$.

Using the high-resolution diphoton and ZZ channels discussed above, we obtain the 68% CL contours for the signal strength versus mass shown at left in Figure 8. To extract the mass in a model-independent way, the individual signal yields are allowed to vary independently within their uncertainties. The combined best-fit mass is 125.3 ± 0.4 (stat) ± 0.5 (syst) GeV. The signal strengths and uncertainties for each of the five channels are depicted at right in Figure 8. The overall combined signal strength, including all channels, is 0.87 ± 0.23 , consistent, within the relatively large uncertainties, with the expectations for the SM Higgs boson. The data rule out the SM Higgs boson in the ranges 114.4–121.5 GeV and 128–600 GeV at 95% CL [20].

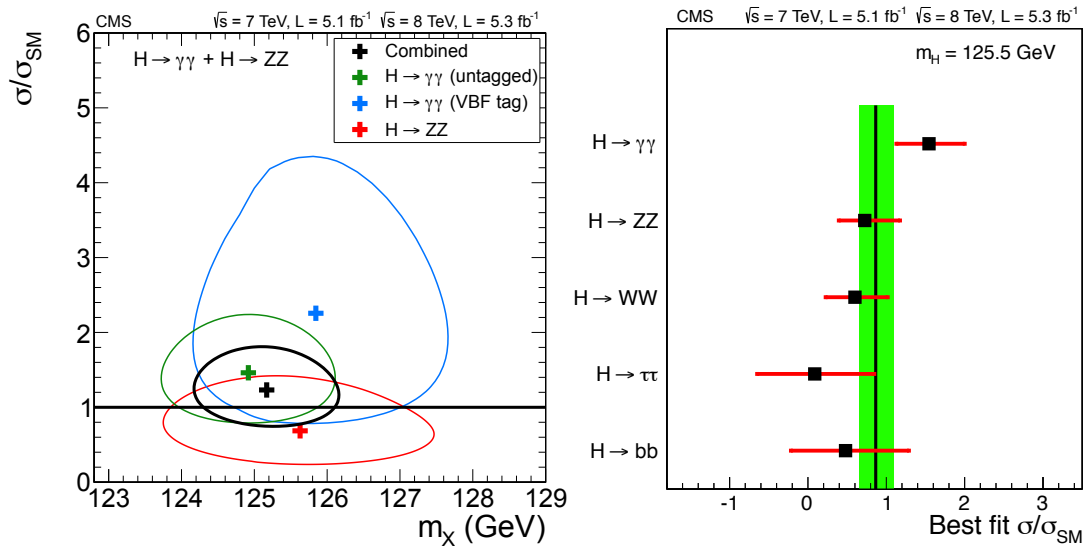


Fig. 8: Left: 68% confidence level contours for the relative signal strength σ/σ_{SMH} versus mass of the new particle (denoted X) for $H \rightarrow \gamma\gamma$ and ZZ . Right: σ/σ_{SMH} for the five decay modes examined by CMS.

More data are needed to establish whether or not this new particle has all the observable properties expected for the SM Higgs boson. Significant discrepancies would point to new physics beyond the SM. The new particle could be a portal to a new landscape of physical phenomena that is still hidden from us. The CMS experiment will continue to study this particle for many years to come.

Acknowledgements

We congratulate our colleagues in the CERN accelerator departments for the excellent performance of the LHC machine. We thank the computing centers in the Worldwide LHC Computing Grid for the provisioning and excellent performance of computing infrastructure essential to our analyses. We gratefully acknowledge the contributions of the technical and administrative staffs at CERN and other CMS institutes. Finally we acknowledge the support from all the funding agencies that enabled the construction and operation of the CMS detector: BMWF and FWF (Austria); FNRS and FWO (Belgium); CNPq, CAPES, FAPERJ, and FAPESP (Brazil); MES (Bulgaria); CERN; CAS, MoST, and NSFC (China); COLCIENCIAS (Colombia); MSES (Croatia); RPF (Cyprus); MEYS (Czech Republic); MoER, SF0690030s09 and ERDF (Estonia); Academy of Finland, MEC, and HIP (Finland); CEA and CNRS/IN2P3 (France); BMBF, DFG, and HGF (Germany); GSRT (Greece); OTKA and NKTH (Hungary); DAE and DST (India); IPM (Iran); SFI (Ireland); INFN (Italy); NRF and WCU (Korea); LAS (Lithuania); CINVESTAV, CONACYT, SEP, and UASLPFAI (Mexico); MSI (New Zealand); PAEC (Pakistan); MSHE and NSC (Poland); FCT (Portugal); JINR (Armenia, Belarus, Georgia, Ukraine, Uzbekistan); MON, RosAtom, RAS and RFBR (Russia); MSTD (Serbia); SEIDI and CPAN (Spain); Swiss Funding Agencies (Switzerland); NSC (Taipei); TUBITAK and TAEK (Turkey); NASU (Ukraine); STFC (United Kingdom); DOE and NSF (USA).

References

- [1] S.L. Glashow, *Partial-symmetries of weak interactions*, Nucl. Phys. **22** (1961) 579, doi:10.1016/0029-5582(61)90469-2.
- [2] S. Weinberg, *A Model of Leptons*, Phys. Rev. Lett. **19** (1967) 1264, doi:10.1103/PhysRevLett.19.1264.
- [3] A. Salam, *Weak and electromagnetic interactions*, in Elementary particle physics: relativistic groups and analyticity, N. Svartholm, ed., p. 367. Almqvist & Wiskell, 1968, Proceedings of the eighth Nobel symposium.
- [4] F. Englert and R. Brout, *Broken symmetry and the mass of gauge vector mesons*, Phys. Rev. Lett. **13** (1964) 321, doi:10.1103/PhysRevLett.13.321.
- [5] P.W. Higgs, *Broken symmetries, massless particles and gauge fields*, Phys. Lett. **12** (1964) 132, doi:10.1016/0031-9163(64)91136-9.
- [6] P.W. Higgs, *Broken symmetries and the masses of gauge bosons*, Phys. Rev. Lett. **13** (1964) 508, doi:10.1103/PhysRevLett.13.508.
- [7] G.S. Guralnik, C.R. Hagen, and T.W.B. Kibble, *Global conservation laws and massless particles*, Phys. Rev. Lett. **13** (1964) 585, doi:10.1103/PhysRevLett.13.585.
- [8] P.W. Higgs, *Spontaneous symmetry breakdown without massless bosons*, Phys. Rev. **145** (1966) 1156, doi:10.1103/PhysRev.145.1156.
- [9] T.W.B. Kibble, *Symmetry breaking in non-Abelian gauge theories*, Phys. Rev. **155** (1967) 1554, doi:10.1103/PhysRev.155.1554.
- [10] J. M. Cornwall, D. N. Levin, and G. Tiktopoulos, *Uniqueness of spontaneously broken gauge theories*, Phys. Rev. Lett. **30** (1973) 1268, doi:10.1103/PhysRevLett.30.1268

- [11] J. M. Cornwall, D. N. Levin, and G. Tiktopoulos, *Derivation of gauge invariance from High-Energy Unitarity Bounds on the s Matrix*, Phys. Rev. D **10** (1974) 1145, doi:10.1103/PhysRevD.10.1145. Also erratum, doi:10.1103/PhysRevD.11.972.
- [12] C. H. Llewellyn Smith, *High-Energy Behaviour and Gauge Symmetry*, Phys. Lett. B **46** (1973) 233, doi:10.1016/0370-2693(73)90692-8.
- [13] B. W. Lee, C. Quigg, and H. B. Thacker, *Weak Interactions at Very High-Energies: The Role of the Higgs Boson Mass*, Phys. Rev. D **16** (1977) 1519, doi:10.1103/PhysRevD.16.1519.
- [14] ALEPH, DELPHI, L3, OPAL Collaborations, and LEP Working Group for Higgs Boson Searches, *Search for the Standard Model Higgs boson at LEP*, Phys. Lett. B **565** (2003) 61, doi:10.1016/S0370-2693(03)00614-2., arXiv:hep-ex/0306033.
- [15] CDF and D0 Collaborations, *Combination of Tevatron Searches for the Standard Model Higgs Boson in the W^+W^- Decay Mode*, Phys. Rev. Lett. **104** (2010) 061802, doi:10.1103/PhysRevLett.104.061802. A more recent, unpublished, limit is given in preprint arXiv:1207.0449.
- [16] CDF Collaboration, *Combined search for the standard model Higgs boson decaying to a bb pair using the full CDF data set*, Phys.Rev.Lett. **109** (2012) 111802, doi:10.1103/PhysRevLett.109.111802, arXiv:1207.1707.
- [17] CDF and D0 Collaborations, *Evidence for a particle produced in association with weak bosons and decaying to a bottom-antibottom quark pair in Higgs boson searches at the Tevatron*, Phys. Rev. Lett. **109** (2012) 071804, doi:10.1103/PhysRevLett.109.071804.
- [18] D0 Collaboration, *Combined search for the standard model Higgs boson decaying to bb using the D0 Run II data set*, Phys. Rev. Lett. (2012), submitted for publication, arXiv:1207.6631.
- [19] L. Evans, P. Bryant (editors), *LHC Machine*, JINST **03** (2008) S08001, doi:10.1088/1748-0221/3/08/S08001
- [20] CMS Collaboration, *Observation of a new boson at a mass of 125 GeV with the CMS Experiment at the LHC* Phys. Lett. B **716** (2012) 30, doi:10.1016/j.physletb.2012.08.021. arXiv:1207.7235
- [21] CMS Collaboration, *The CMS experiment at the CERN LHC*, JINST **03** (2008) S08004, doi:10.1088/1748-0221/3/08/S08004.
- [22] J.R. Ellis, M.K. Gaillard, D.V. Nanopoulos, *A phenomenological profile of the Higgs boson*, Nucl. Phys. B **106** (1976) 292, doi:10.1016/0550-3213(76)90382-5.
- [23] H.M. Georgi, S.L. Glashow, M.E. Machacek, D.V. Nanopoulos, *Higgs Bosons from Two Gluon Annihilation in Proton Proton Collisions*, Phys. Rev. Lett. **40** (1978) 692, doi:10.1103/PhysRevLett.40.692.
- [24] S.L. Glashow, D.V. Nanopoulos, A. Yildiz, *Associated Production of Higgs Bosons and Z Particles*, Phys. Rev. D **18** (1978) 1724, doi:10.1103/PhysRevD.18.1724.
- [25] S. Alioli, P. Nason, C. Oleari, E. Re, *NLO Higgs boson production via gluon fusion matched with shower in POWHEG*, JHEP **04** (2009) 002, doi:10.1088/1126-6708/2009/04/002.
- [26] P. Nason, C. Oleari, *NLO Higgs boson production via vector boson fusion matched with shower in POWHEG*, JHEP **02** (2010) 037, doi:10.1007/JHEP02(2010)037.
- [27] T. Sjöstrand, S. Mrenna, P.Z. Skands, *PYTHIA 6.4 physics and manual*, JHEP **05** (2006) 026, doi:10.1088/1126-6708/2006/05/026.

- [28] S. Gieseke, D. Grellscheid, K. Hamilton, A. Ribon, P. Richardson, et al., *Herwig++ 2.0 Release Note (2006)*, arXiv:hep-ph/0609306.
- [29] J. Alwall, P. Demin, S. de Visscher, R. Frederix, M. Herquet, et al., *MadGraph/MadEvent v4: the new web generation*, JHEP **09** (2007) 028, doi:10.1088/1126-6708/2007/09/028, arXiv:0706.2334.
- [30] S. Agostinelli, et al., *GEANT4—a simulation toolkit*, Nucl. Instrum. Meth. A **506** (2003) 250, doi:10.1016/S0168-9002(03)01368-8.
- [31] CMS Collaboration, *Combined results of searches for the Standard Model Higgs boson in pp collisions at $\sqrt{s} = 7$ TeV*, Phys. Lett. B **710** (2012) 26, doi:10.1016/PhysLettB.2012.02.064, arXiv:1202.1488.
- [32] CMS Collaboration, *Search for the Standard Model Higgs boson decaying into two photons in pp collisions at $\sqrt{s} = 7$ TeV*, Phys. Lett. B **710** (2012) 403, doi:10.1016/j.physletb.2012.03.003, arXiv:1202.1487.
- [33] CMS Collaboration, *Search for the Standard Model Higgs boson in the decay channel $H \rightarrow ZZ \rightarrow 4l$ in pp collisions at $\sqrt{s} = 7$ TeV*, Phys. Rev. Lett. **108** (2012) 111804, doi:10.1103/PhysRevLett.108.111804, arXiv:1202.1997.
- [34] CMS Collaboration, *Search for the Standard Model Higgs boson decaying to W^+W^- in the fully leptonic final state in pp collisions at $\sqrt{s} = 7$ TeV*, Phys. Lett. B **710** (2012) 91, doi:10.1016/j.physletb.2012.02.076, arXiv:1202.1489.
- [35] CMS Collaboration, *Search for neutral Higgs bosons decaying to tau pairs in pp collisions at $\sqrt{s} = 7$ TeV*, Phys. Lett. B **713** (2012) 68, doi:10.1016/j.physletb.2012.05.028, arXiv:1202.4083.
- [36] CMS Collaboration, *Search for the Standard Model Higgs boson decaying to bottom quarks in pp collisions at $\sqrt{s} = 7$ TeV*, Phys. Lett. B **710** (2012) 284, doi:10.1016/j.physletb.2012.02.085, arXiv:1202.4195.
- [37] ATLAS Collaboration, *Combined search for the Standard Model Higgs boson in pp collisions at $\sqrt{s} = 7$ TeV with the ATLAS detector*, (2012), Phys. Rev. D **86** (2012) 032003, doi:10.1103/PhysRevD.86.032003, arXiv:1207.0319.
- [38] H. B. Prosper, *Multivariate methods in particle physics: Today and tomorrow*, 2008, PoS ACAT08 (2008) 010.
- [39] P. C. Bhat, *Multivariate Analysis Methods in Particle Physics*, Ann. Rev. Nucl. Part. Sci. **61** (2011) 281-309.
- [40] L. D. Landau, *The moment of a 2-photon system*, Dokl. Akad. Nauk **60** (1948) 207.
- [41] C. N. Yang, *Selection Rules for the Dematerialization of a Particle Into Two Photons*, Phys. Rev. **77** (1950) 242, doi:10.1103/PhysRev.77.242.
- [42] CMS Collaboration, *Search for a Higgs boson in the decay channel $H \rightarrow ZZ \rightarrow qqll^+$ in pp collisions at $\sqrt{s} = 7$ TeV*, JHEP **04** (2012) 036, doi:10.1007/JHEP04(2012)036, arXiv:1202.1416.
- [43] CMS Collaboration, *Z inclusive cross-section via decays to tau pairs at 7 TeV*, JHEP **08** (2011) 117, doi:10.1007/JHEP08(2011)117, arXiv:1104.1617.
- [44] ATLAS and CMS Collaborations, *LHC Higgs Combination Group, Procedure for the LHC Higgs boson search combination in Summer 2011*, Tech. Rep. ATL-PHYS-PUB 2011-11, CMS NOTE 2011/005 (2011). URL: <http://cdsweb.cern.ch/record/1379837>.